Early involvement of cellular stress and inflammatory signals in the pathogenesis of tubulointerstitial kidney disease due to *UMOD* mutations

Matteo Trudu[1], Celine Schaeffer[1], Michela Riba[2], Masami Ikehata[3,4], Paola Brambilla[5], Piergiorgio Messa[3,4], Filippo Martinelli-Boneschi[5], Maria Pia Rastaldi[3], Luca Rampoldi[1*]

SUPPLEMENTARY INFORMATION

Supplementary Figures 1-6, Supplementary Table 1

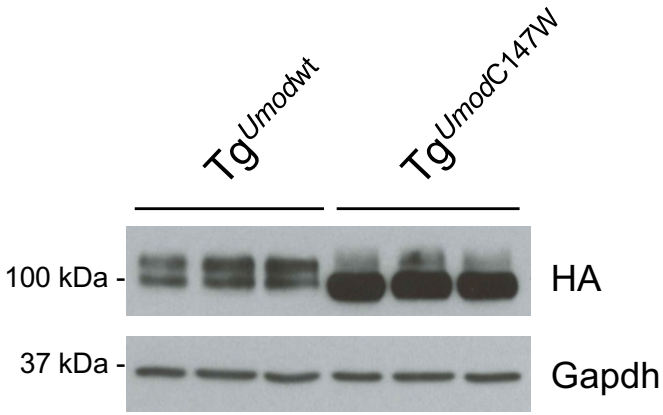

Supplementary Figure 1. Western blot analysis showing expression of HA-tagged transgenic uromodulin in kidneys of 1 month-old Tg$^{Umod\text{wt}}$ and Tg$^{Umod\text{C147W}}$ mice. The figure shows cropped blot images (full blots are reported in **Supplementary Figure 6**). Mutant uromodulin is strongly retained in the ER, as demonstrated by the accumulation of the lower molecular weight isoform, corresponding to uromodulin ER precursor. Gapdh was used as loading control.

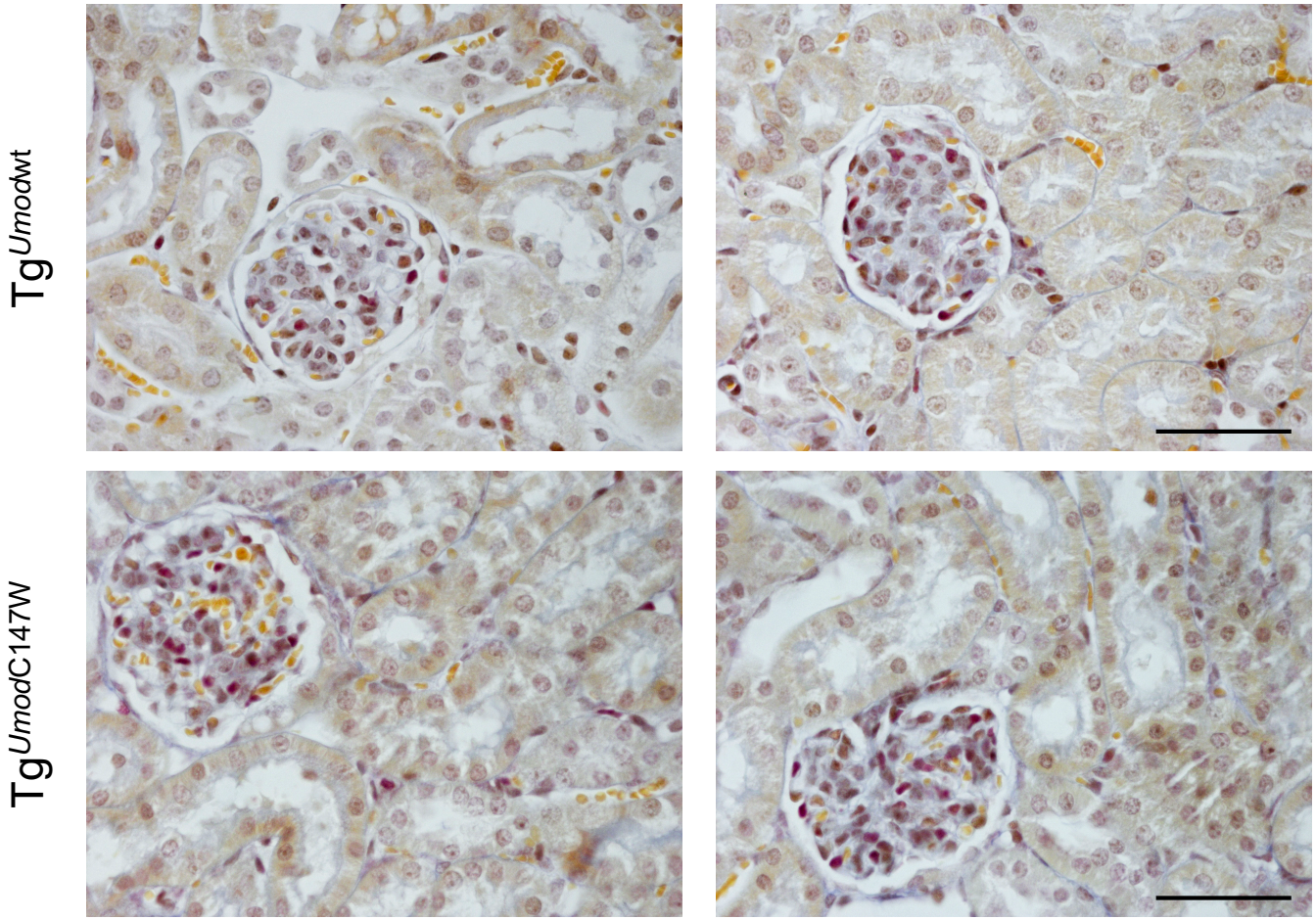

Supplementary Figure 2. Representative histological images of glomeruli in kidneys of 1 month-old Tg*Umod*C147W and Tg*Umod*wt (AFOG; scale bar 50 µm). Quantification of mesangial hypercellularity, mesangial matrix expansion and focal/segmental glomerulosclerosis showed no difference between Tg*Umod*C147W and Tg*Umod*wt mice (data not shown, n = 9 Tg*Umod*wt and 6 Tg*Umod*C147W).

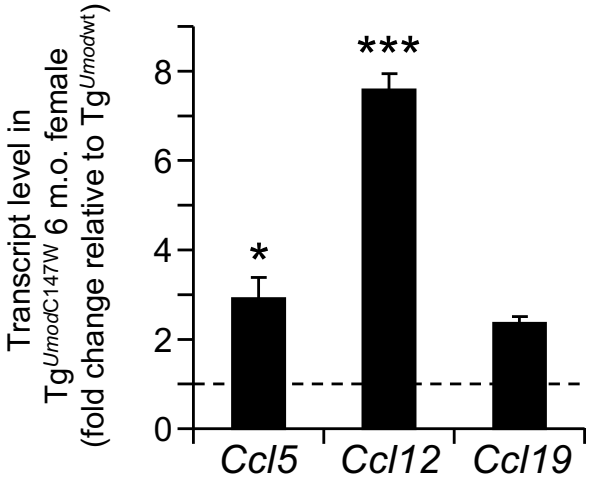

Supplementary Figure 3. Analysis by real-time RT-qPCR of the expression of selected chemokines in 6 month-old Tg$^{Umod\text{C147W}}$ mice relative to age- and sex-matched Tg$^{Umod\text{wt}}$ (n = 5/group). Data are expressed as mean ± s.e.m. *P < 0.05; ***P < 0.001 (unpaired t-test).

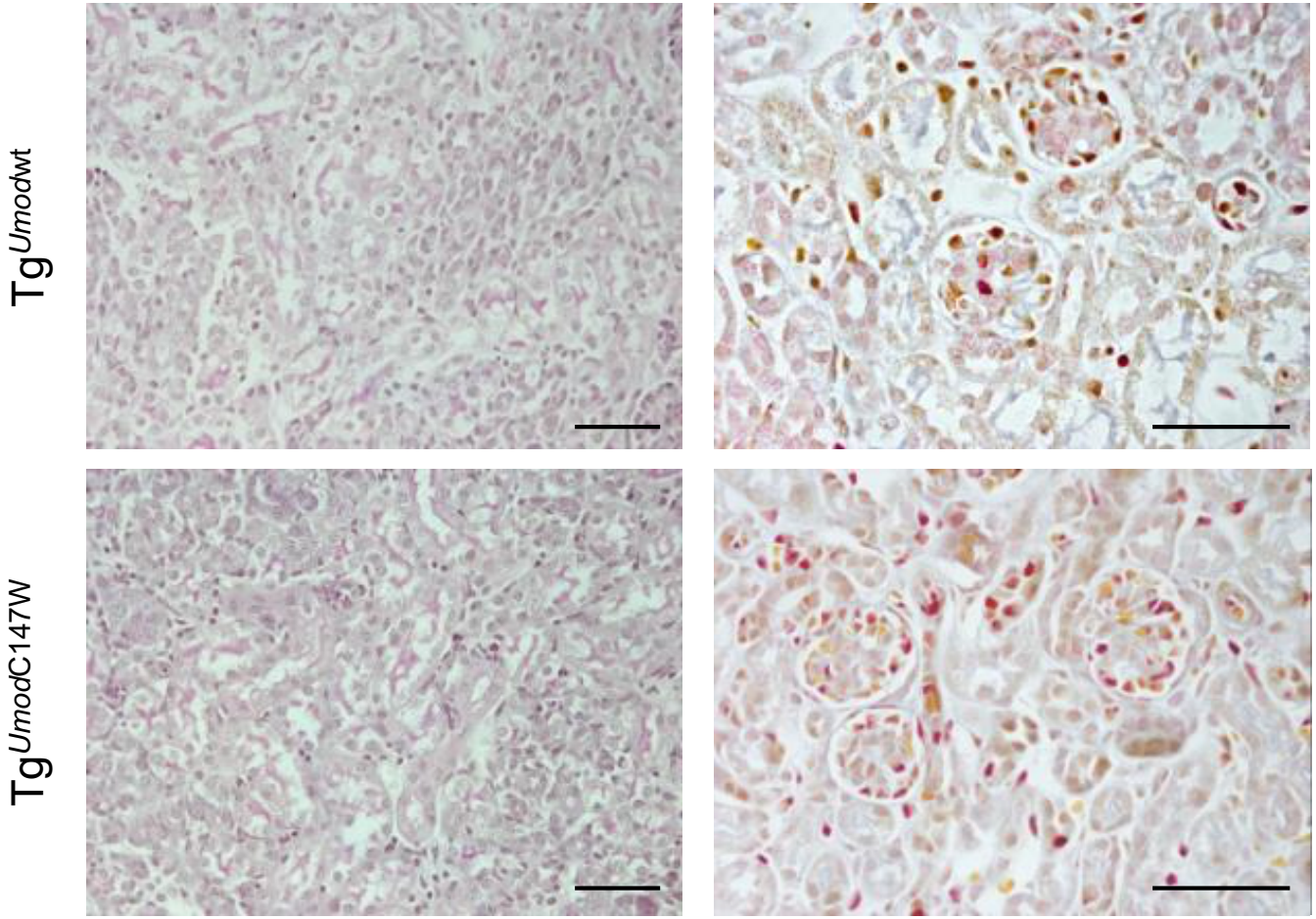

Supplementary Figure 4. Representative histological images of tubular architecture and glomeruli in kidneys of Tg$^{Umod\mathrm{C147W}}$ and Tg$^{Umod\mathrm{wt}}$ mice at p8 (PAS, left panels, and AFOG, right panels; scale bar 50 µm). Quantification of tubular casts, tubular damage, interstitial inflammation, interstitial fibrosis, mesangial hypercellularity, mesangial matrix expansion and focal/segmental glomerulosclerosis showed no difference between Tg$^{Umod\mathrm{C147W}}$ and Tg$^{Umod\mathrm{wt}}$ mice (data not shown, n = 4/group).

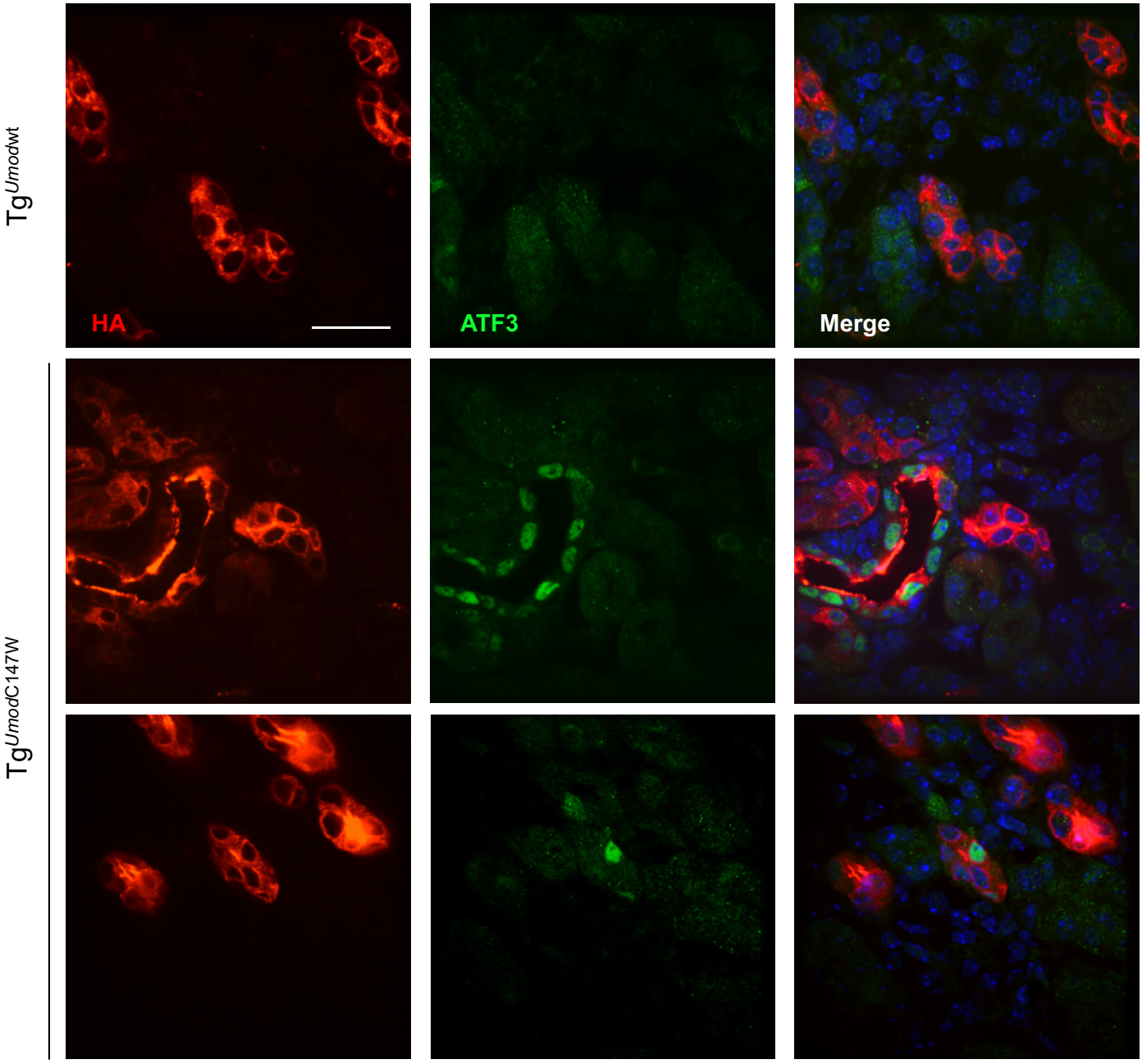

Supplementary Figure 5. Expression of Atf3 in the kidneys of p8 transgenic mice. Immunofluorescence analysis reveals that Atf3 is specifically detected in nuclei of TAL segments in kidneys of Tg*Umod*C147W mice (scale bar 15 µm).

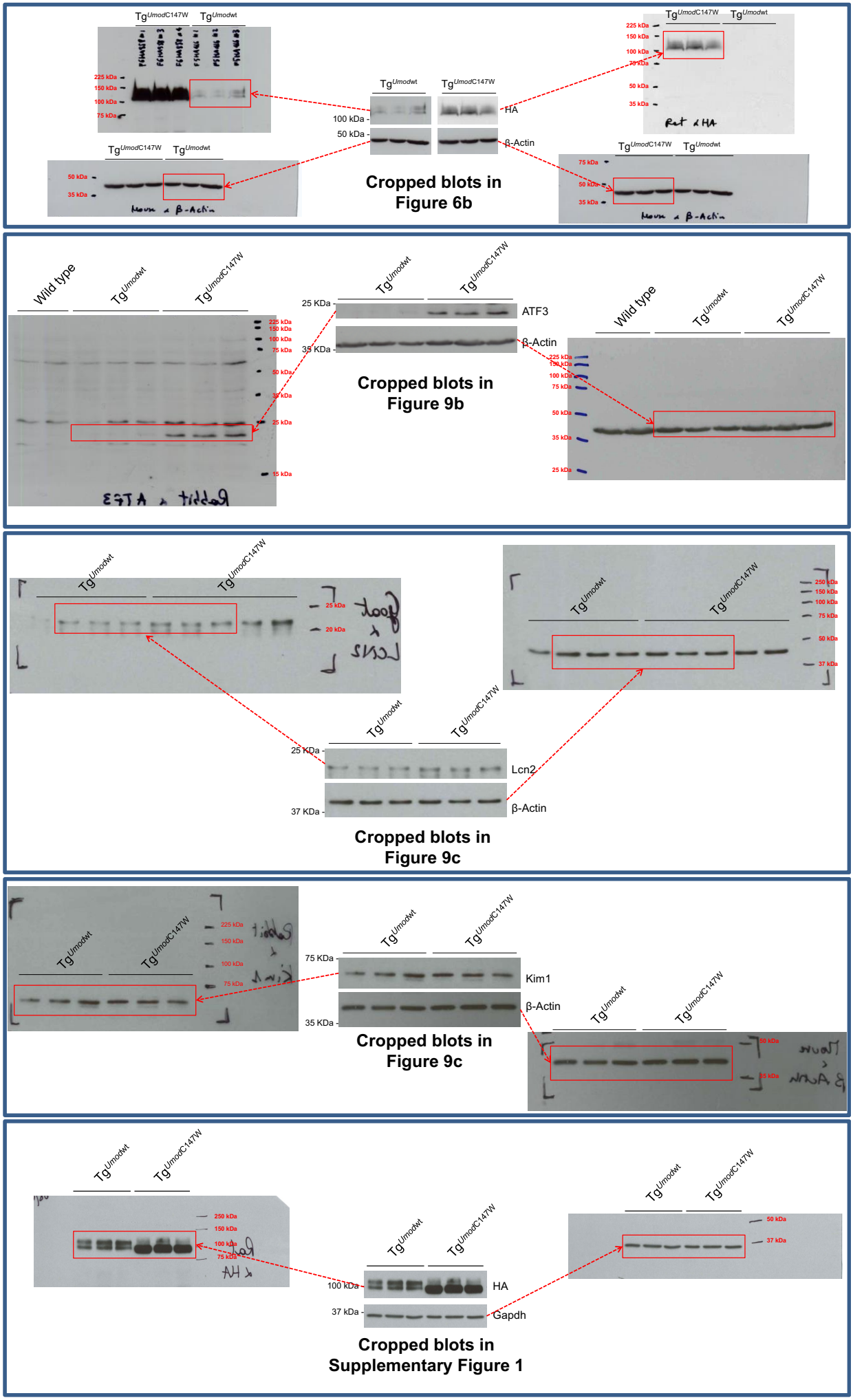

Supplementary Figure 6. Full image of blots shown as cropped images in **Figure 6b**, **Figure 9b**, **Figure 9c**, **Supplementary Figure 1**. The red boxes indicate the cropped images.

Supplementary Table 1. List of primers used for SYBR Green real-time RT-qPCR.

Target gene	Forward primer (5'-3')	Reverse primer (5'-3')
Ccl5	GTGCCCACGTCAAGGAGTATT	CCCACTTCTTCTCTGGGTTGG
Ccl12	CATCAGTCCTCAGGTATTGGCTGGA	CTTGGGGTCAGCACAGATCTCCTT
Ccl19	CTGGCCTTCAGCCTGCTGGT	TGCGATCCACCCAGGGCTGG
Tgfb1	CCCGCGTGCTAATGGTGGACC	TGCACGGGACAGCAATGGGG
Vim	GGATCAGCTCACCAACGACA	GGTCAAGACGTGCCAGAGAA
Col6a1	ACCGACTGCGCCATTAAGAA	GTCGGTCACCACGATCAAGT
Acta2	GCTACGAACTGCCTGACGG	GCTGTTATAGGTGGTTTCGTGGA
Acox3	GCTCACTTCACAAGCCCTCT	TAGCAAACAAGCCAGCGGTA
Ehhadh	GCCATAGTGATCTGTGGAGCA	ACCACTGGCTTCTGGTATCG
Cyp4b1	CCAGCTCAGCAAGCCAGTAA	GTGGGTCAAAGACCTCTGGG
Col1a1	CTGACGCATGGCCAAGAAGA	ATACCTCGGGTTTCCACGTC
Ntn4	AGGATTTTCTGCCCTCCGAC	ATGGGAGCCTTTGTCGTGG
Panx1	GCTCATCTCGCTGGCCTTCGC	AATCCACAAAGGCAGCCTGTCGC
Slc13a3	TATGGTGGAATGAGCTGGAGA	GGCAAACGTGCAGAACAAGAT
Slc25a17	GCCTCTGTGCTGTCCTACG	ACCTGAAGCCGAAGTCTAGC
Cd5	CCCTTGCCAATTCGATGGGA	GGGCTGGAAATCAGAGCAGA
Cd19	ACCAGTTGGCAGGATGATGG	GCTGAGGAGCTGCATAGAGG
Ptprc	GGAGACCAGGAAGTCTGTGC	GTTCTGGGCTCCTTCCTCTT
Cd68	CTGACAAGGGACACTTCGGG	AGGCCAATGATGAGAGGCAG
Fut4	GAGGTGGGTGTGGATGAACT	GTTGGATCGCTCCTGGAATA
Lcn2	TCCCCCTGCAGCCAGACTTCC	AGTAGCGACAGCCCTGGTCCTG
Havcr1	TTGGCATCTGCATCGCAGCCC	GGGAATGCACAACCGCTGCGT
Atf3	CAGAAGTCAGTGCGACCGCC	TCGCCGCCTCCTTTTCCTCTCA
Hprt1	ACATTGTGGCCCTCTGTGTG	TTATGTCCCCCGTTGACTGA